Comparator Networks

Weidi Xie, Li Shen and Andrew Zisserman

Visual Geometry Group, Department of Engineering Science,
University of Oxford
{weidi,lishen,az}@robots.ox.ac.uk

Abstract. The objective of this work is set-based verification, e.g. to decide if two sets of images of a face are of the same person or not. The traditional approach to this problem is to learn to generate a feature vector per image, aggregate them into *one* vector to represent the set, and then compute the cosine similarity. Instead, we design a neural network architecture that can directly learn set-based verification.
Our contributions are: (i) We propose a Deep Comparator Network (DCN) that can ingest a pair of sets (each may contain a *variable* number of images) as inputs, and learns the similarity function by attending to multiple discriminative local regions (landmarks), and comparing the set-based local descriptors in pairs; (ii) To encourage high-quality representations for set, an internal competition mechanism is introduced for dynamic recalibration based on the landmark score confidence; (iii) Inspired by image retrieval, a novel hard sample mining regime is proposed to control the sampling process, such that the DCN is complementary to the standard classification models trained with a single image. Evaluations on the IARPA Janus face recognition benchmarks show that the comparator networks outperform the previous state-of-the-art results by a large margin.

1 Introduction

The objective of this paper is to determine if two sets of images are of the same object or not. For example, in the case of face verification, the set could be images of a face; and in the case of person re-identification, the set could be images of the entire person. In both cases the objective is to determine if the sets show the same person or not.

In the following, we will use the example of sets of faces, which are usually referred to as 'templates' in the face recognition literature, and we will use this term from here on. A template could consist of multiple samples of the same person (e.g. still images, or frames from a video of the person, or a mixture of both). With the great success of deep learning for image classification [1–4], by far the most common approach to template-based face verification is to use a deep convolutional neural network (CNN) to generate a vector representing each face, and simply average these vectors to obtain a vector representation for the template [5–8]. Verification then proceeds by comparing the template vectors. Rather than improve on this simple combination rule, the research drives until now has been to improve the performance of the single image representation

by more sophisticated training losses, such as Triplet Loss, PDDM, and Histogram Loss [6, 7, 9–12]. This approach has achieved very impressive results on the challenging benchmarks, such as the IARPA IJB-B and IJB-C datasets [13, 14].

However, this procedure of first generating a single vector per face, and then simply averaging these, misses out on potentially using more available informaton in four ways:

First, *viewpoint conditioned similarity* – it is easier to determine if two faces are of the same person or not when they have a similar pose and lighting. For example, if both are frontal or both in profile, then point to point comparison is possible, whereas it isn't if one is in profile and the other frontal;

Second, *local landmark comparison* – to solve the fine-grained problem, it is essential to compare discriminative congruent 'parts' (local regions of the face) such as an eye with an eye, or a nose with a nose.

Third, *within template weighting* – not all images in a template are of equal importance, the features derived from a low resolution or blurred face is probably of less importance than the ones coming from a high-resolution perfectly focussed face;

Fourth, *between template weighting* – what is useful for verification depends on what is in both templates. For example if one template has only profile faces, and the second is all frontal apart from one profile instance, then it is likely that the single profile instance in the second template is of more importance than the frontal ones.

The simple average combination rule cannot take advantage of any of these four – for example, unweighted average pooling ignores the difference in the amount of information provided by each face image. In fact the template vector will be restricted to the convex hull of its constituent face vectors [15], and an abherrant image, such as one that is quite blurred, can have a significant effect (since most blurred face images look similar).

In this paper, we introduce a *Deep Comparator Network* (DCN), a network architecture designed to compare pairs of templates. The model consists of three modules: *Detect, Attend* and *Compare*, as illustrated in Figure 1, that address the four requirements above: in the *Detect* module, besides the dense feature representation maps, multiple discriminative landmark detectors act on each input image and generate the score maps; the *Attend* module normalizes the landmark responses over the images within template, and output multiple landmark specific feature descriptors by using image specific weighted average pooling on the feature maps, finally, the *Compare* module compares these landmark specific feature vectors between the two templates, and aggregates into *one* vector for final similarity prediction. The DCN can handle any number of images in a template, and is trained end-to-end for the task of template verification. The network is described in detail in § 3.

As a second contribution we introduce an idea from the instance retrieval literature to face template verification. Large scale instance retrieval systems achieved superior results by proceeding in two stages: given a query image, images are first retrieved and ranked using a very efficient method, such as bag

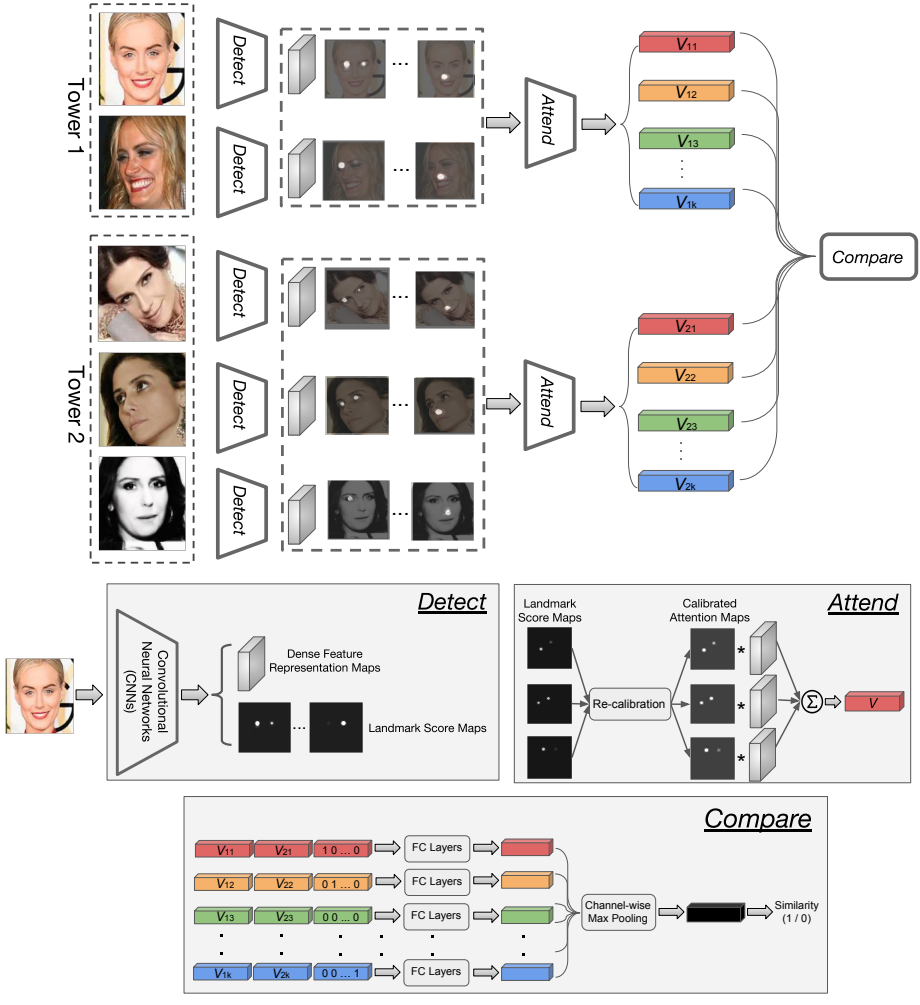

Fig. 1. *Top*: overview of the Deep Comparator Network (DCN)
Bottom: functionality of the individual modules, namely, *Detect*, *Attend*, *Compare*. Each of the two towers in the DCN, is able to take a template (with an arbitrary number of images) as input. Each image is fed into a shared *Detect* module and outputs a feature map, as well as multiple discriminative landmark score maps. In the *Attend* module, landmark score maps (predicted from the same filter on different input images) are first re-calibrated within the template, and then landmark specific feature responses for each template are obtained by weighted average pooling on the feature maps. In the *Compare* module, landmark specific feature responses between the two templates are compared with local "experts" (parametrized as fully conneted layers), and aggregated into *one* vector for final similarity prediction.

of visual words; then, in a second stage, the top k images are re-ranked using a more expensive method, such as geometric consistency with the query [16, 17]. Since image classification models can be trained very efficiently nowadays, we re-purpose this re-ranking idea for template verification as follows: during training, we employ a standard classification model (pre-trained on single image classification) for sampling the hard template pairs, such that we can explicitly control the verification difficulty level, and focus on the template pairs that single-image classification model can not deal with. This is described in § 4, together with other training details, such as the training set and loss functions. In § 5, we report the verification performance of the DCN on the challenging IARPA Janus face recognition benchmarks – IJB-B [13] and IJB-C [14]. In both datasets, the DCN is able to *substantially* outperform the previous state-of-the-art methods.

2 Related work

In this section we review the work that has influenced the design of the DCN.
Multi-column architectures. Recent works [18, 19] extend the traditional image-wise architectures to multi-columns, where the models are designed to take a set of images/frames as inputs, and produce a single vector representation for the entire template. The model is trained to fuse useful information from the multiple inputs based on the image "quality"; for instance, high-resolution, frontal faces are weighted more than faces under extreme imaging conditions or poses. However, these models still try to encode the entire template with *one* vector, and are trained with standard classification losses. They still cannot tackle the challenge of *local landmark comparison* and *between template weightings*.

Face recognition based on part representations. Several previous works proposed to use part-based representation for a single face image or face tacks. In [20], the face image is densely partitioned into overlapping patches at multiple scales, and each of the patches is represented by local features, such as Local Binary Pattern (LBP) or SIFT, then represented as a bag of spatial-appearance features by clustering. In [21], a Fisher Vector (FV) encoding is used to aggregate local features across different video frames to form a video-level representation. As shown in the paper, each Gaussian component acts as a dense pseudo-part detector that is invariant to face pose and identity, thus, the comparison of those Fisher vectors can be seen as an implicit and robust comparison of face parts.

Attention models. Attention models have been successfully used in machine translation [22], multiple object recognition [23], and image captioning [24]. In [25], the authors propose to extract part-based feature representations from a single input image with attention, and perform fine-grained classifications with these part specific representations. In general, the idea of these attentional pooling can be seen as a generalization of average or max pooling, where the spatial weights are parametrized as a function (usually a small neural network) mapping from input image to an attentional mask. Apart from soft attention, [26] proposed the Spatial Transformer Networks (STNs) that allows to learn whichever

transformation parameters best aid the classification task. Although no ground truth transformation is specified during training, the model still implicitly learns to attend and focus on the object of interest. Recent work [27] proposed to use the STNs recursively to localize multiple facial parts from the input image. However, this approach tends to be sensitive to image quality – in the template-based recognition problems, the STNs will potentially zoom into wrong regions if the image quality is low, and therefore contribute noisy features to the templates.

Relation/co-occurrence learning. In [28], in order to perform the spatial relational reasoning, the features at every spatial location are concatenated and modelled with the features at every other locations, To model the co-occurence statistics of features, e.g. "brown eyes", bilinear CNNs [29] was proposed and experimented on the fine-grained classification problems, the descriptor of one image is obtained from the outer product of the feature maps. As for the few-shot learning, in [30], the authors propose to map a small labelled support set and an unlabelled example to its labels by learning a similarity metric with the deep neural features. As an extension, [31] experiments with more powerful representations, where the feature maps of images (from support set and test set) are concatenated and passed to a relation module for similarity learning. Similarly, in this paper, we parameterize local "experts" to compare the feature vectors from two sets.

3 Deep Comparator Networks

We consider the task of template-based verification, where the objective is to decide if two given templates are of the same object or not. Generally, in verification problems the label spaces of the training set and testing set are disjoint. In the application considered here, the images are of faces, and the objective is to verify whether two templates show the same person or not. The identities in the test set are not seen during training.

From a high-level viewpoint, Deep Comparator Network (DCN) focus on the scenario that two tenplates (each has an arbitrary number of images) are taken as inputs, and trained end-to-end for template verification. A DCN consists of three modules (as illustrated in Figure 1): *Detect*, *Attend* and *Compare*, to address the four challenges, i.e. *viewpoint conditioned similarity, local landmark comparison, within and between template weighting*. We first overview the function of these modules, and then give more details of their implementation. A detailed description of the architecture of the individual modules is given in the supplementary material.

The *Detect* module is shared for each input image, and a dense feature representation map, as well as multiple discriminative part score maps are outputted, in the face recognition literature, these discriminative parts are usually termed "landmarks", we will use this term from here on. Note that, the implicitly inferred landmarks aim to best assist the subsequent template verification task, they may not follow the same intuitions as human defined facial landmarks, e.g. a mouth corner. Given a template with multiple images in various poses or

illuminations, the landmark filters will be sensitive to different facial parts, viewpoints, or illuminations, e.g. one may be sensitive to the eyes in a frontal face, one may be more responsive to a mouth in a profile face. The *Detect* module acts as the base for fullfilling template comparison conditioned on *viewpoints/local landmarks*.

The *Attend* module achieves the *within template weighting* with an internal competition mechanism, and pools out multiple landmark specific feature descriptors for each template. Given a template with multiple images, we hope to emphasize the feature representations from the relatively high quality images, while suppressing the contribution from the low ones. To achieve this, we recalibrate the score maps (inferred from different samples with the same landmark filter) into a probability distribution. Consequently, multiple landmark specific feature descriptors are calculated by attending to the feature maps with image specific attentional masks. Therefore, the viewpoint factors and facial parts are decomposed and template-wise aligned.

Finally, we use the *Compare* module to achieve the *between template weighting*. The template-wise verification is reformulated as the comparison conditioned on both global and local regions (i.e. landmarks), votings from the local "experts" are aggregated into *one* vector for the final similarity prediction.

3.1 Detect

The *Detect* module inputs an image, and generates an intermediate dense representation and multiple (K) landmark score maps. Formally, we parametrize the module as a standard 40-layer ResNet ($\psi(\cdot;\theta_1)$) with outputs for n images (Figure 2 shows an example where $n = 3$):

$$[F_1, F_2, ..., F_n, A_1, A_2, ..., A_n] = [\psi(I_1;\theta_1), \psi(I_2;\theta_1), ..., \psi(I_n;\theta_1)] \quad (1)$$

where each input image is of size $I \in R^{W\times H\times 3}$, the output dense feature representation map $F \in R^{\frac{W}{8}\times\frac{H}{8}\times C}$, and a *set* of attention maps $A \in R^{\frac{W}{8}\times\frac{H}{8}\times K}$, where W, H, C, K refer to the width, height, channels, and the number of landmark score maps respectively. Note here, each of the score maps (A's) is the results of *linear convolutions*. A global score map is also obtained by a max over the local landmark score maps.

Ideally, the local score maps for each image should satisfy two conditions, *first*, they should be mutally exclusive (i.e. at each spatial location only one landmark is activated); *second*, the scores on the maps should positively correlate with image quality, e.g. the response of a particular landmark filter should be higher on high-resolution frontal images than on low-resolution frontal images. Indeed the experimental results corrobate that this is so.

3.2 Attend

Dynamic Re-calibration (Internal Competition). Given the feature maps and landmark score maps for each input image, cross-normalization is used among the score maps within same template for *dynamic re-calibration*. Based on the

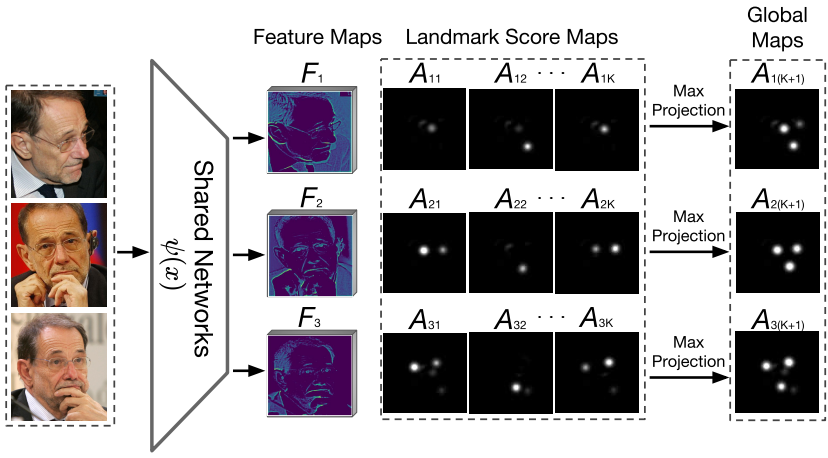

Fig. 2. The detect module. For each input image the detect module generates an intermediate feature map ($F's$), K landmark attention maps ($A's$), and a global map (obtained by applying a max on the $A's$ channel dimension). In this example there are three input images and three of the K landmark attention maps are shown. .

"quality" of images within the tower, the score maps (from different images within a single template) that localize same landmark are normalized as a distribution of weightings. Therefore, no matter how many images are packed into a template, the outputted attention maps in the same column always add up to 1.0 (Figure 1). Formally, for every $n \in [1, N]$ and $k \in [1, K]$:

$$A_{n..k} = \frac{exp(A_{n..k})}{\sum_{nij} exp(A_{nijk})} \tag{2}$$

Attentional Pooling. With the re-calibrated attention maps for each input image, we next attend to the spatial locations and compute representations by image specific weighted averaging over the entire template. Formally, for each of the input image ($n \in N$), with the feature map as F_n, and one set of attention maps A_n,

$$V_k = \sum_{nij} F_{nij:} \odot A_{nijk} \qquad \text{for } k \in [1 : K+1] \tag{3}$$

Therefore, for each input template, we are able to calculate $K+1$ feature descriptors (K landmark specific descriptors, "1" global feature descriptor), with each feature descriptor representing either one of the facial landmarks or global information.

3.3 Compare

Up to this point, we have described how to pool $K+1$ feature vectors from the single template. In this module, we compare these descriptors in pairs between two different templates. In detail, the landmark specific feature descriptors from two templates are first L2 normalized, and concatenated along with a one-hot encoded landmark identifier. Each concatenated vector is the input to a local "expert" modelled by a fully connected (FC) layers [28]. Overall, the local experts are responsible for comparing the landmark specific feature respones from different templates.

Formally, we learn a similarity function $y = C(x; \theta_2)$, where $x = [V_{1k} : V_{2k} : \mathrm{ID}_{one\text{-}hot}]$, as shown in Figure 1. After passing through the fully connected layers, the feature representations given by local "experts" are max pooled, and fused to provide the final similarity score.

Discussion. Unlike the approach of [29, 28], where features at every spatial location are compated with features at every other location, the compare module here only compares the descriptors that encode the same landmark, e.g. frontal mouth to frontal mouth. By attaching the landmark identifier (the one-hot indicator vector), the fully connected layers are able to specialize for each landmark.

4 Experimental details

4.1 VGGFace2 Dataset

In this paper, all models are trained with the large-scale VGGFace2 dataset [5]. In total, the dataset contains about 3.31 million images with large variations in pose, age, illumination, ethnicity and profession (e.g. actors, athletes, politicians). Approximately, 362.6 images exist for each of the 9131 identities on average. The entire dataset is divided into the training set (8631 identities) and validation set (500 identities). In order to be comparable with other existing models, we follow the same dataset split and train the models with only 8631 identities.

4.2 Landmark Regularizers

In the *Attend* module, the landmark score maps can be considered as a generalization of global average pooling, where the spatial "weights" are inferred implicitly based on the input image. However, in the *Detect* module, there is nothing to prevent the network from learning K identical copies of the same landmark, for instance, it can learn to always predict the average pooling mask, or detect the eyes, or given a network with large enough receptive field, it can always pinpoint the centre of the image. To prevent this, we experiment with two different types of landmark regularizers: a diversity regularizer and a keypoints regularizer.

Diversity Regularizer. In order to encourage landmark diversity, the most obvious approach is to penalize the mutual overlap between the score maps of different landmarks. We use the same method as [32]. Each of the landmark score maps is first self-normalized into a probability distribution (p's) by using the softmax (Eq 4),

$$p_{nijk} = \frac{exp(A_{nijk})}{\sum_{ij} exp(A_{nijk})} \tag{4}$$

where n, i, j, k refer to the image index within the template, width, height, number of attention maps respectively.

Ideally, if all K landmarks are disjoint from each other, by taking the max projection of these normalized distribution, there should be exactly K landmarks, and they should sum to K.

$$\mathcal{L}_{reg} = nK - \sum_{nij} \max_{k=1,..,K} p_{nijk} \tag{5}$$

Note here, this regularizer is zero only if the activations in the different normalized landmark score maps are disjoint and exactly 1.0.

Keypoints Regularizer. Benifiting from the previous fruitful research in facial keypoint detection, pseudo groundtruth for the landmarks can be obtained from pre-trained facial keypoint detectors. Although the facial keypoint predictions are not perfect, we conjecture that they are sufficiently accurate to guide the network training at the early stages, and, as the training progresses, the regularizer weights is scheduled to decay, gradually releasing the parameter search space. As preprocessing, we predict 5 facial keypoints (Figure 3) over the entire dataset with a pre-trained MTCNN [33], and estimate three face poses by thresholding angle ratios.[1]

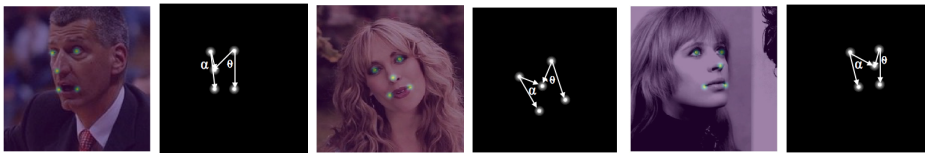

Fig. 3. Facial landmark detection for VGGFace2 images.
Face poses are quantized into three categories based on the ration α/θ. Left-facing profile : $\alpha/\theta < 0.3$, right-facing profile: $\alpha/\theta > 3.0$, frontal face: $\alpha/\theta \in [0.3, 3.0]$

Similar to the diveristy regularizer, the inferred landmark score maps are also self-normalized first (Eq 4), and the $\mathcal{L}2$ loss between the prediction (p) and

[1] In our training, we only use 4 facial landmarks, left-eye, right-eye, nose, mouth. The mouth landmarks are obtained by averaging the two landmarks at mouth corners.

the pseudo groundtruth ($\hat{p}$) is applied as auxiliary supervision. Note that, given each face image belongs to only one of the three poses, only 4 of the 12 landmark map are actually useful for supervising an individual image.

$$\mathcal{L}_{reg} = \begin{cases} \sum_{nij} \frac{1}{2}(p_{nijk} - \hat{p}_{nijk})^2 \text{ for k in } \{\text{pose-specific keypoints}\} \\ 0 \end{cases} \tag{6}$$

To make the experiments comparable, in both experiments, we use $K = 12$ landmark score maps in the *Detect* module.

4.3 Loss Functions

The proposed comparator network is trained end-to-end by optimizing three types of losses simultaneously: *first*, template-level identity classification softmax loss, using a global feature representation obtained by attentional pooling with the re-calibrated global maps (refer to Figure 2); *second*, a standard classification loss (2 classes) on the similarity score prediction from the *Compare* module; *third*, a regularization loss from the landmark score maps in the *Detect* module.

$$\mathcal{L} = \alpha_1(\mathcal{L}_{cls1} + \mathcal{L}_{cls2}) + \alpha_2\mathcal{L}_{sim} + \alpha_3\mathcal{L}_{reg} \tag{7}$$

where $\alpha_1 = 2.0, \alpha_2 = 5.0$ refer to the loss weights for classification and similarity prediction, α_3 refers to the weights for regularizer, which was initialized as 30.0 and decayed by half every $60,000$ iterations. Note that, α_3 is scheduled to decrease, thus, even for the training with the keypoints regularizer, the auxiliary supervision only guides the network training in early stages.

4.4 Hard-sample Mining

In order to train the Comparator Network for re-ranking we require a method to sample hard template-template pairs. Here we described the procedure for this. The key idea is to use the features generated by a standard ResNet-50 trained for face image classification (on the VGGFace2 training set) to approximate the template descriptor, and use this approximate template descriptor to select hard template pairs. Note, these templates are hard relative to the ResNet-50 trained for single image face classification. In detail, the template-level descriptors are obtained by averaging the feature vectors (pre-computed from ResNet-50) of 3 images and L2-normalized.

The selection of hard template pairs is then integrated into the training of the comparator network. At each iteration 256 identities are randomly sampled, and used to create 512 templates with 3 images in each template (i.e. two templates for each identity). In total, there are therefore 256 positive template pairs, and a large number of negative pairs.

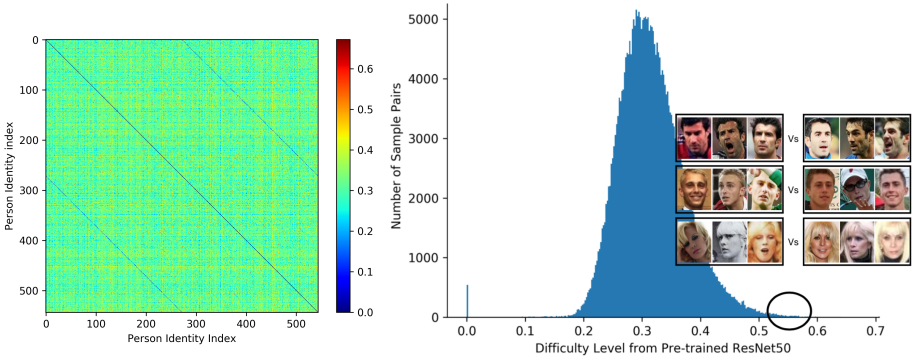

(a) Confusion matrix (b) Sampling histogram

Fig. 4. Sampling strategy based on the pre-trained single-image classification networks. Larger values refer to more difficult template pairs. The Comparator Network is trained by sampling template pairs at different levels.

By calculating the cosine similarity between different pairs of templates, we generate a 512×512 similarity matrix M_s for the template-to-template verification, where small values refer to the predicted dissimilar pairs from the pre-trained ResNet50. We further define the verification difficulty matrix as:

$$d = |groundtruth - M_s| \tag{8}$$

where groundtruth label is either 0 (dissimilar) or 1 (similar). Therefore, in the difficulty matrix, the small values refer to the easy sample pairs, and the large values refer to the difficult samples. Based on this difficulty matrix, we are able to sample the training samples that cover the very difficult template pairs that the pre-trained ResNet-50 can not distinguish (Figure 4).

4.5 Training details

We train the entire Comparator Network end-to-end from scratch on the VGGFace2 dataset. In the *Detect* module, a simple ResNet [3] with 40 layers is shared across the two towers, images are passed through until the width and height of the feature maps is 1/8 of the original resolution. During training, the shorter side of the input image is resized to 144, while the long side is center cropped, making the input images 144×144 pixels with the face centered, and 127.5 is subtracted from each channel. In each tower, 3 images are packed as a template input. Note that, there is a probability of 20% that the 3 images within one template are identical images[2]. In this case, the Comparator Network become equivalent to training on single image. Data augmentation is operated

[2] This guarantees a probability of 64% that both templates contain 3 different images, and a probability of 36% that at least one template contains 3 identical image.

separately with probability of 20%, including flipping, gaussian blur, motion blur, monochrome transformation. Adam [34] was used for optimization with an initial learning rate as $1e^{-4}$, and mini-bateches of size 64, with equal number of positive and negative pairs. The learning rate is decreased twice with a factor of 10 when errors plateau. Note that, although the batch size is small, the network is actually seeing 64×6 images every training step. Also, although the network is only trained with 3 images per tower, at test time it can be applied to any number of images per template.

5 Results

We evaluate all models on the challenging IARPA Janus Benchmarks, where all images and videos are captured from unconstrained environments and show large variations in viewpoints and image quality. Note, in contrast to the traditional closed-world classification tasks (where the identities are the same during training and testing), verification is an open-world problem (i.e. the label spaces of the training and test set are disjoint), and thus challenges the capacity and generalization of the feature representations.

We evaluate the models on the standard 1:1 verification protocol (matching between the Mixed Media probes and two galleries), the performance is reported as the true accept rates (TAR) vs. false positive rates (FAR) (i.e. receiver operating characteristics (ROC) curve). During testing, we first report the results from only DCN, however, note that, in order to align with the re-ranking process during training, the DCN should ideally be used along with models trained with single image.

IJB-B Dataset [13] The IJB-B dataset is an extension of IJB-A [35], having $1,845$ subjects with 21.8K still images (including $11,754$ face and $10,044$ non-face) and 55K frames from $7,011$ videos.

Model	1:1 Verification TAR			
	FAR=$1E-4$	FAR=$1E-3$	FAR=$1E-2$	FAR=$1E-1$
Whitelam *et al.* [13]	0.540	0.700	0.840	– –
Navaneeth *et al.* [36]	0.685	0.830	0.925	0.978
ResNet50 [5]	0.784	0.878	0.938	0.975
SENet50 [5]	0.800	0.888	0.949	0.984
DCNs(Kpts)	0.823	0.921	0.966	0.991
DCNs(Divs)	0.835	0.923	0.971	0.995
ResNet50+SENet50	0.800	0.887	0.946	0.981
ResNet50+DCN(Kpts)	**0.850**	0.927	0.970	0.992
ResNet50+DCN(Divs)	0.841	0.930	0.972	0.995
SENet50+DCN(Kpts)	0.846	0.935	0.974	0.997
SENet50+DCN(Divs)	0.849	**0.937**	**0.975**	**0.997**

Table 1. Evaluation on 1:1 verification protocol on IJB-B dataset. (Higher is better)
Note that the result of Navaneeth *et al.* [36] was on the Janus CS3 dataset.
DCN(Divs) : Deep Comparator Network trained with Diversity Regularizer
DCN(Kpts): Deep Comparator Network trained with Keypoints Regularizer.

IJB-C Dataset [14] The IJB-C dataset is a further extension of IJB-B, having 3,531 subjects with 31.3K still images and 117.5K frames from 11,779 videos. In total, there are 23124 templates with 19557 genuine matches and 15639K impostor matches.

Model	1:1 Verification TAR			
	FAR=$1E-4$	FAR=$1E-3$	FAR=$1E-2$	FAR=$1E-1$
GOTS-1 [14]	0.160	0.320	0.620	0.800
FaceNet [14]	0.490	0.660	0.820	0.920
VGG-CNN [14]	0.600	0.750	0.860	0.950
ResNet50 [5]	0.825	0.900	0.950	0.980
SENet50 [5]	0.840	0.910	0.960	0.987
DCNs(Kpts)	0.851	0.921	0.969	0.992
DCNs(Divs)	0.862	0.930	0.972	0.994
ResNet50+SENet50	0.841	0.909	0.957	0.985
ResNet50+DCN(Kpts)	0.867	0.940	0.979	0.997
ResNet50+DCN(Divs)	0.880	0.944	0.981	0.998
SENet50+DCN(Kpts)	0.874	0.944	0.981	0.998
SENet50+DCN(Divs)	**0.885**	**0.947**	**0.983**	**0.998**

Table 2. Evaluation on 1:1 verification protocol on IJB-C dataset. (Higher is better) Results of GOTS-1, FaceNet, VGG-CNN are read from ROC curve in [14].

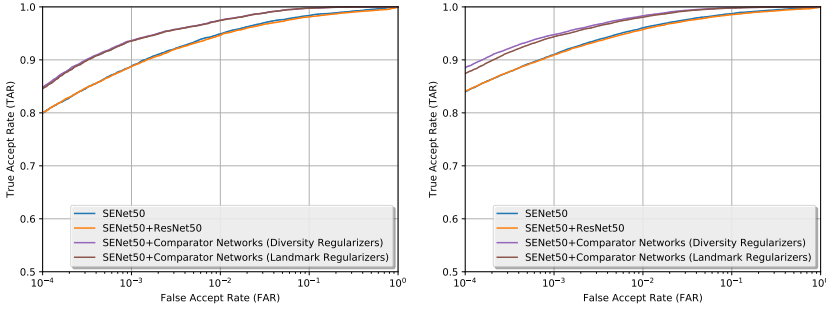

(a) ROC for IJB-B (Higher is better) (b) ROC for IJB-C (Higher is better)

Fig. 5. ROC curve of 1:1 verification protocol on IJB-B & IJB-C dataset.

5.1 Discussion

Three phenomena can be observed from the evaluation results: *first*, comparing the previous state-of-the-art model [5], the DCN trained by re-ranking can boost the performance significantly on both IJBB and IJBC (about $4-5\%$, which is a substantial reduction in the error); *second*, although the ResNet50 and SENet50 are designed differently and trained separately, ensembles of them do not provide any benifit (the performance even drops slightly). This shows that the difficult template pairs for ResNet50 remains difficult for another more powerful SENet50, showing that the models trained on single image classification are not complementary to each other; while in contrast, the DCN can be used together with either ResNet50 or SENet50 to improve the recognition system; *third*, the performance of DCN trained with different regularizers are comparable to each other, showing that groundtruth of facial keypoints is not critical in training DCN.

5.2 Visualization

Figure 6 shows the attention maps for a randomly sampled template that contains multiple images with varying poses. Visualizing the maps in this way makes the models interpretable, as it can be seen what the landmark detectors are concentrating on when making the verification decision. The *Detect* module has learnt to pinpoint the landmarks in different poses consistently, and is even tolerant to some out-of-plane rotation. Interestingly, the landmark detector actually learns to localize the two eyes simultaneously; we conjecture, that this is due to the fact that human faces are approximately symmetric, and also during training, the data is augmented with horizontal flippings.

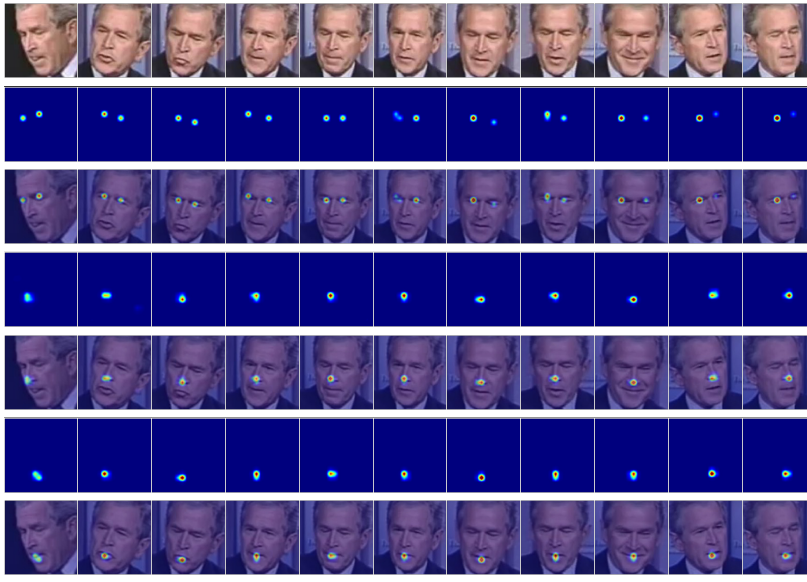

Fig. 6. Predicted facial landmark score maps after self-normalizing for three of the landmark detectors. Additional examples are given in the supplementary material. *1st row*: raw images in the template, faces in a variaty of poses are shown from left to right; *2nd,4th,6th row*: self-normalized landmark score maps (attention maps); *3rd, 5th, 7th row*: images overlayed with the attention maps.

6 Conclusion

We have introduced a new network that is able to compare templates of images to verify if they match or not, and demonstrated its use on face template verification. The network is very *flexible*, in that the number of images in each template can be varied at test time, it is also *opportunistic* in that it can take advantage of local evidence at test time, such as a specific facial features like a tattoo or a port-wine stain that might be lost in a traditional single tower per face encoding. Its performance substantially improves the state-of-the-art on the recent and very challenging IJB benchmarks.

Although we have used face templates in this work, the Comparator Network could also potentially be applied to other fine-grained classification, e.g. to determine the species of a bird or flower from multiple images of the same instance.

Acknowledgment

This research is based upon work supported by the Office of the Director of National Intelligence (ODNI), Intelligence Advanced Research Projects Activity (IARPA), via contract number 2014-14071600010. The views and conclusions contained herein are those of the authors and should not be interpreted as necessarily representing the official policies or endorsements, either expressed or implied, of ODNI, IARPA, or the U.S. Government. The U.S. Government is authorized to reproduce and distribute reprints for Governmental purpose notwithstanding any copyright annotation thereon.

References

1. Krizhevsky, A., Sutskever, I., Hinton, G.E.: ImageNet classification with deep convolutional neural networks. In: NIPS. (2012) 1106–1114
2. Simonyan, K., Zisserman, A.: Very deep convolutional networks for large-scale image recognition. In: ICLR. (2015)
3. He, K., Zhang, X., Ren, S., Sun, J.: Deep residual learning for image recognition. In: Proc. CVPR. (2016)
4. Hu, J., Shen, L., Sun, G.: Squeeze-and-excitation networks. arXiv preprint arXiv:1709.01507 (2017)
5. Cao, Q., Shen, L., Xie, W., Parkhi, O.M., Zisserman, A.: VGGFace2: A dataset for recognising faces across pose and age. In: Intl. Conf. Automatic Face and Gesture Recognition (FG) (2018), http://www.robots.ox.ac.uk/ vgg/data/vgg_face2/
6. Parkhi, O.M., Vedaldi, A., Zisserman, A.: Deep face recognition. In: Proc. BMVC. (2015)
7. Schroff, F., Kalenichenko, D., Philbin, J.: Facenet: A unified embedding for face recognition and clustering. In: Proc. CVPR. (2015)
8. Taigman, Y., Yang, M., Ranzato, M., Wolf, L.: Deepface: Closing the gap to human-level performance in face verification. In: Proc. CVPR. (2014)
9. Schultz, M., Joachims, T.: Learning a distance metric from relative comparisons. In: NIPS. (2004)
10. Weinberger, K.Q., Blitzer, J., Saul, L.: Distance metric learning for large margin nearest neighbor classification. In: NIPS. (2006)
11. Ustinova, E., Lempitsky, V.: Learning deep embeddings with histogram loss. In: NIPS. (2016)
12. Hermans, A., Beyer, L., Leibe, B.: In Defense of the Triplet Loss for Person Re-Identification. arXiv preprint arXiv:1703.07737 (2017)
13. Whitelam, C., Taborsky, E., Blanton, A., Maze, B., Adams, J., Miller, T., Kalka, N., Jain, A.K., Duncan, J.A., Allen, K., et al.: IARPA janus benchmark-b face dataset. In: CVPR Workshop on Biometrics. (2017)
14. Maze, B., Adams, J., Duncan, J.A., Kalka, N., Miller, T., Otto, C., Jain, A.K., Niggel, W.T., Anderson, J., Cheney, J., Grother, P.: IARPA janus benchmark-c: Face dataset and protocol. In: 11th IAPR International Conference on Biometrics. (2018)

15. Cevikalp, H., Triggs, B.: Face recognition based on image sets. In: Proc. CVPR. (2010)
16. Philbin, J., Chum, O., Isard, M., Sivic, J., Zisserman, A.: Object retrieval with large vocabularies and fast spatial matching. In: Proc. CVPR. (2007)
17. Jégou, H., Douze, M., Schmid, C.: Hamming embedding and weak geometric consistency for large scale image search. In: Proc. ECCV. (2008) 304–317
18. Luan, T., Xi, Y., Xiaoming, L.: Disentangled representation learning gan for pose-invariant face recognition. In: Proc. CVPR. (2017)
19. Yang, J., Ren, P., Zhang, D., Chen, D., Wen, F., Li, H., Hua, G.: Neural aggregation network for video face recognition. In: Proc. CVPR. (2017)
20. Li, H., Hua, G., Brandt, J., Yang, J.: Probabilistic elastic matching for pose variant face verification. In: Proc. CVPR. (2013)
21. Parkhi, O.M., Simonyan, K., Vedaldi, A., Zisserman, A.: A compact and discriminative face track descriptor. In: Proc. CVPR. (2014)
22. Bahdanau, D., Cho, K., Bengio, Y.: Neural machine translation by jointly learning to align and translate. Proc. ICLR (2015)
23. Ba, J., Mnih, V., Kavukcuoglu, K.: Multiple object recognition with visual attention. Proc. ICLR (2015)
24. Xu, K., Ba, J., Kiros, R., Cho, K., Courville, A., Salakhudinov, R., Zemel, R., Bengio, Y.: Show, attend and tell: Neural image caption generation with visual attention. In: Proc. ICML. (2015)
25. Zheng, H., Fu, J., Mei, T., Luo, J.: Learning multi-attention convolutional neural network for fine-grained image recognition. In: Proc. ICCV. (2017)
26. Jaderberg, M., Simonyan, K., Zisserman, A., et al.: Spatial transformer networks. In: NIPS. (2015)
27. Wu, W., Kan, M., Liu, X., Yang, Y., Shan, S., Chen, X.: Recursive spatial transformer (rest) for alignment-free face recognition. In: Proc. ICCV. (2017)
28. Santoro, A., Raposo, D., Barrett, D.G.T., Malinowski, M., Pascanu, R., Battaglia, P., Lillicrap, T.P.: A simple neural network module for relational reasoning. CoRR **abs/1706.01427** (2017)
29. Lin, T.J., RoyChowdhury, A., Maji, S.: Bilinear cnn models for fine-grained visual recognition. In: Proc. ICCV. (2015)
30. Vinyals, O., Blundell, C., Lillicrap, T., kavukcuoglu, k., Wierstra, D.: Matching networks for one shot learning. In: NIPS. (2016)
31. Sung, F., Yang, Y., Zhang, L., Xiang, T., Torr, P.H.S., Hospedales, T.M.: Learning to compare: Relation network for few-shot learning. In: Proc. CVPR. (2018)
32. Thewlis, J., Bilen, H., Vedaldi, A.: Unsupervised learning of object llandmarks by factorized spatial embeddings. In: Proc. ICCV. (2017)
33. Zhang, K., Zhang, Z., Li, Z., Qiao, Y.: Joint face detection and alignment using multitask cascaded convolutional networks. IEEE Signal Processing Letters **23**(10) (2016) 1499–1503
34. Kingma, D.P., Ba, J.: Adam: A method for stochastic optimization. CoRR **abs/1412.6980** (2014)
35. Klare, B.F., Klein, B., Taborsky, E., Blanton, A., Cheney, J., Allen, K., Grother, P., Mah, A., Jain, A.K.: Pushing the frontiers of unconstrained face detection and recognition: IARPA janus benchmark a. In: Proc. CVPR. (2015)
36. Navaneeth, B., Jingxiao, Z., Hongyu, X., Jun-Cheng, C., Carlos, C., Rama, C.: Deep heterogeneous feature fusion for template-based face recognition. In: IEEE Winter Conference on Applications of Computer Vision, WACV. (2017)